

Measurement of D^* Production in Jets from $\bar{p}p$ Collisions at $\sqrt{s} = 1.8$ TeV

F. Abe,⁽¹⁶⁾ D. Amidei,⁽³⁾ G. Apollinari,⁽¹¹⁾ G. Ascoli,⁽⁷⁾ M. Atac,⁽⁴⁾ P. Auchincloss,⁽¹⁴⁾ A. R. Baden,⁽⁶⁾ A. Barbaro-Galtieri,⁽⁹⁾ V. E. Barnes,⁽¹²⁾ F. Bedeschi,⁽¹¹⁾ S. Behrends,⁽¹²⁾ S. Belforte,⁽¹¹⁾ G. Bellettini,⁽¹¹⁾ J. Bellinger,⁽¹⁷⁾ J. Bensinger,⁽²⁾ A. Beretvas,⁽¹⁴⁾ P. Berge,⁽⁴⁾ S. Bertolucci,⁽⁵⁾ S. Bhadra,⁽⁷⁾ M. Binkley,⁽⁴⁾ R. Blair,⁽¹⁾ C. Blocker,⁽²⁾ J. Boffill,⁽⁴⁾ A. W. Booth,⁽⁴⁾ G. Brandenburg,⁽⁶⁾ D. Brown,⁽⁶⁾ A. Byon,⁽¹²⁾ K. L. Byrum,⁽¹⁷⁾ M. Campbell,⁽³⁾ R. Carey,⁽⁶⁾ W. Carithers,⁽⁹⁾ D. Carlsmith,⁽¹⁷⁾ J. T. Carroll,⁽⁴⁾ R. Cashmore,⁽⁴⁾ F. Cervelli,⁽¹¹⁾ K. Chadwick,^{(4),(12)} T. Chapin,⁽¹³⁾ G. Chiarelli,⁽¹¹⁾ W. Chinowsky,⁽⁹⁾ S. Cihangir,⁽¹⁵⁾ D. Cline,⁽¹⁷⁾ D. Connor,⁽¹⁰⁾ M. Contreras,⁽²⁾ J. Cooper,⁽⁴⁾ M. Cordelli,⁽⁵⁾ M. Curatolo,⁽⁵⁾ C. Day,⁽⁴⁾ R. DelFabbro,⁽¹¹⁾ M. Dell'Orso,⁽¹¹⁾ L. DeMortier,⁽²⁾ T. Devlin,⁽¹⁴⁾ D. DiBitonto,⁽¹⁵⁾ R. Diebold,⁽¹⁾ F. Dittus,⁽⁴⁾ A. DiVirgilio,⁽¹¹⁾ J. E. Elias,⁽⁴⁾ R. Ely,⁽⁹⁾ S. Errede,⁽⁷⁾ B. Esposito,⁽⁵⁾ B. Flaughner,⁽¹⁴⁾ E. Focardi,⁽¹¹⁾ G. W. Foster,⁽⁴⁾ M. Franklin,^{(6),(7)} J. Freeman,⁽⁴⁾ H. Frisch,⁽³⁾ Y. Fukui,⁽⁸⁾ A. F. Garfinkel,⁽¹²⁾ P. Giannetti,⁽¹¹⁾ N. Giokaris,⁽¹³⁾ P. Giromini,⁽⁵⁾ L. Gladney,⁽¹⁰⁾ M. Gold,⁽⁹⁾ K. Goulianos,⁽¹³⁾ C. Grosso-Pilcher,⁽³⁾ C. Haber,⁽⁹⁾ S. R. Hahn,⁽¹⁰⁾ R. Handler,⁽¹⁷⁾ R. M. Harris,⁽⁹⁾ J. Hauser,⁽³⁾ T. Hessing,⁽¹⁵⁾ R. Hollebeek,⁽¹⁰⁾ P. Hu,⁽¹⁴⁾ B. Hubbard,⁽⁹⁾ P. Hurst,⁽⁷⁾ J. Huth,⁽⁴⁾ H. Jensen,⁽⁴⁾ R. P. Johnson,⁽⁴⁾ U. Joshi,⁽¹⁴⁾ R. W. Kadel,⁽⁴⁾ T. Kamon,⁽¹⁵⁾ S. Kanda,⁽¹⁶⁾ D. A. Kardelis,⁽⁷⁾ I. Karliner,⁽⁷⁾ E. Kearns,⁽⁶⁾ R. Kephart,⁽⁴⁾ P. Kesten,⁽²⁾ H. Keutelian,⁽⁷⁾ S. Kim,⁽¹⁶⁾ L. Kirsch,⁽²⁾ K. Kondo,⁽¹⁶⁾ U. Kruse,⁽⁷⁾ S. E. Kuhlmann,⁽¹²⁾ A. T. Laasanen,⁽¹²⁾ W. Li,⁽¹⁾ T. Liss,⁽³⁾ N. Lockyer,⁽¹⁰⁾ F. Marchetto,⁽¹⁵⁾ R. Markeloff,⁽¹⁷⁾ L. A. Markosky,⁽¹⁷⁾ P. McIntyre,⁽¹⁵⁾ A. Menzione,⁽¹¹⁾ T. Meyer,⁽¹⁵⁾ S. Mikamo,⁽⁸⁾ M. Miller,⁽¹⁰⁾ T. Mimashi,⁽¹⁶⁾ S. Miscetti,⁽⁵⁾ M. Mishina,⁽⁸⁾ S. Miyashita,⁽¹⁶⁾ N. Mondal,⁽¹⁷⁾ S. Mori,⁽¹⁶⁾ Y. Morita,⁽¹⁶⁾ A. Mukherjee,⁽⁴⁾ C. Newman-Holmes,⁽⁴⁾ L. Nodulman,⁽¹⁾ R. Paoletti,⁽¹¹⁾ A. Para,⁽⁴⁾ J. Patrick,⁽⁴⁾ T. J. Phillips,⁽⁶⁾ H. Piekarz,⁽²⁾ R. Plunkett,⁽¹³⁾ L. Pondrom,⁽¹⁷⁾ J. Proudfoot,⁽¹⁾ G. Punzi,⁽¹¹⁾ D. Quarrie,⁽⁴⁾ K. Ragan,⁽¹⁰⁾ G. Redlinger,⁽³⁾ J. Rhoades,⁽¹⁷⁾ F. Rimondi,⁽⁴⁾ L. Ristori,⁽¹¹⁾ T. Rohaly,⁽¹⁰⁾ A. Roodman,⁽³⁾ A. Sansoni,⁽⁵⁾ R. Sard,⁽⁷⁾ V. Scarpine,⁽⁷⁾ P. Schlabach,⁽⁷⁾ E. E. Schmidt,⁽⁴⁾ P. Schoessow,⁽¹⁾ M. H. Schub,⁽¹²⁾ R. Schwitters,⁽⁶⁾ A. Scribano,⁽¹¹⁾ S. Segler,⁽⁴⁾ M. Sekiguchi,⁽¹⁶⁾ P. Sestini,⁽¹¹⁾ M. Shapiro,⁽⁶⁾ M. Sheaff,⁽¹⁷⁾ M. Shibata,⁽¹⁶⁾ M. Shochet,⁽³⁾ J. Siegrist,⁽⁹⁾ P. Sinervo,⁽¹⁰⁾ J. Skarha,⁽¹⁷⁾ D. A. Smith,⁽⁷⁾ F. D. Snider,⁽³⁾ R. St. Denis,⁽⁶⁾ A. Stefanini,⁽¹¹⁾ Y. Takaiwa,⁽¹⁶⁾ K. Takikawa,⁽¹⁶⁾ S. Tarem,⁽²⁾ D. Theriot,⁽⁴⁾ A. Tollestrup,⁽⁴⁾ G. Tonelli,⁽¹¹⁾ Y. Tsay,⁽³⁾ F. Ukegawa,⁽¹⁶⁾ D. Underwood,⁽¹⁾ R. Vidal,⁽⁴⁾ R. G. Wagner,⁽¹⁾ R. L. Wagner,⁽⁴⁾ J. Walsh,⁽¹⁰⁾ T. Watts,⁽¹⁴⁾ R. Webb,⁽¹⁵⁾ T. Westhusing,⁽⁷⁾ S. White,⁽¹³⁾ A. Wicklund,⁽¹⁾ H. H. Williams,⁽¹⁰⁾ T. Yamanouchi,⁽⁴⁾ A. Yamashita,⁽¹⁶⁾ K. Yasuoka,⁽¹⁶⁾ G. P. Yeh,⁽⁴⁾ J. Yoh,⁽⁴⁾ and F. Zetti⁽¹¹⁾

⁽¹⁾Argonne National Laboratory, Argonne, Illinois 60439

⁽²⁾Brandeis University, Waltham, Massachusetts 02254

⁽³⁾University of Chicago, Chicago, Illinois 60637

⁽⁴⁾Fermi National Accelerator Laboratory, Batavia, Illinois 60510

⁽⁵⁾Laboratori Nazionali di Frascati of the Istituto Nazionale di Fisica Nucleare, Italy

⁽⁶⁾Harvard University, Cambridge, Massachusetts 02138

⁽⁷⁾University of Illinois, Urbana, Illinois 61801

⁽⁸⁾National Laboratory for High Energy Physics (KEK), Tsukuba, Ibaraki 305, Japan

⁽⁹⁾Lawrence Berkeley Laboratory, Berkeley, California 94720

⁽¹⁰⁾University of Pennsylvania, Philadelphia, Pennsylvania 19104

⁽¹¹⁾Istituto Nazionale di Fisica Nucleare, University and Scuola Normale Superiore, Pisa, Italy

⁽¹²⁾Purdue University, West Lafayette, Indiana 47907

⁽¹³⁾Rockefeller University, New York, New York 10021

⁽¹⁴⁾Rutgers University, Piscataway, New Jersey 08854

⁽¹⁵⁾Texas A&M University, College Station, Texas 77843

⁽¹⁶⁾University of Tsukuba, Tsukuba, Ibaraki 305, Japan

⁽¹⁷⁾University of Wisconsin, Madison, Wisconsin 53706

(Received 10 October 1989)

The production rate of charged D^* mesons in jets has been measured in 1.8-TeV $\bar{p}p$ collisions at the Fermilab Tevatron with the Collider Detector at Fermilab. In a sample of approximately 32 300 jets with a mean transverse energy of 47 GeV obtained from an exposure of 21.1 nb⁻¹, a signal corresponding to $25.0 \pm 7.5(\text{stat}) \pm 2.0(\text{syst})$ $D^{*\pm} \rightarrow K^\mp \pi^\pm \pi^\pm$ events is seen above background. This corresponds to a ratio $N(D^{*+} + D^{*-})/N(\text{jet}) = 0.10 \pm 0.03 \pm 0.03$ for D^* mesons with fractional momentum z greater than 0.1.

PACS numbers: 13.87.Fh, 14.40.Jz

The multiplicity of heavy quarks in jets can be calculated in perturbative QCD,^{1,2} and the leading nonperturbative correction is believed to be extremely small.² A substantial deviation from the predictions of QCD would therefore be interesting. The UA1 Collaboration has measured the production rate of charged D^* mesons in jets at a center-of-mass energy $\sqrt{s}=546$ GeV.^{3,4} In a measurement based on early data,³ the ratio $N(D^{*\pm})/N(\text{jet})$ was observed to be $0.65 \pm 0.19(\text{stat}) \pm 0.33(\text{syst})$ for D^* 's with fractional momentum $z > 0.1$, where $N(D^{*\pm}) = N(D^{*+} + D^{*-})$. A recent analysis⁴ of later data resulted in the ratio $N(D^{*\pm})/N(\text{jet}) = 0.11 \pm 0.05 \pm 0.02$. In this Letter we present a measurement of D^* production in jets produced at $\sqrt{s}=1.8$ TeV using the Collider Detector at Fermilab (CDF).

The measurement of D^* production in jets from hadronic interactions probes a mechanism different from that in e^+e^- collisions. In e^+e^- collisions the production is dominated by jets initiated by c or b quarks whereas in $\bar{p}p$ collisions one expects to observe D^* 's produced primarily from gluon splitting into $c\bar{c}$ or $b\bar{b}$ pairs.¹ A lowest-order parton-model calculation⁵ indicates that approximately 75% of all jets produced at $\sqrt{s}=1.8$ TeV with transverse energy (E_t) between 40 and 60 GeV, where both jets are in the pseudorapidity⁶ region $|\eta| < 0.8$, come from gluons in the final state, compared to 0.7% from primary c quarks. Thus, even though gluon splitting is a higher-order process, it is expected to be the dominant mechanism for D^* production in jets. A perturbative QCD calculation, including higher-order contributions, predicts the ratio $N(D^{*\pm})/N(\text{jet})$ for 50-GeV gluon jets to be between 0.06 and 0.13, integrated over all values of z .⁷

We mention here briefly those parts of the CDF⁸ most relevant to this study. Vertex time-projection chambers just outside the beam pipe are used to determine the position of the event vertex along the beam direction. Charged-particle momentum information is provided by the central tracking chamber (CTC), which is immersed in a 1.5-T magnetic field and provides full coverage in the pseudorapidity region $|\eta| < 1$. For vertex-constrained tracks, the transverse-momentum resolution is estimated to be $\delta p_t/p_t \approx [(0.0012p_t)^2 + (0.004)^2]^{1/2}$, where p_t is measured in units of GeV/c. The angular resolution is approximately $\delta\phi \approx [(0.3)^2 + (1/p_t)^2]^{1/2}$ mrad in the azimuthal angle and $\delta(\cot\theta) \approx 0.0022$ in the polar angle. These values were obtained for Monte Carlo tracks which were injected into real data. The CTC is surrounded by the central calorimeter, which consists of a lead-scintillator electromagnetic portion followed by a steel-scintillator hadronic compartment. For the jets used in this analysis, the E_t resolution⁹ has an approximately Gaussian shape with a standard deviation (σ) of 8 GeV for 50-GeV jets.

This work is based on an integrated luminosity of 21.1 nb^{-1} ($\pm 15\%$) from a run at the Fermilab Tevatron during which a total of 26.9 nb^{-1} was collected. The

events used in this analysis passed a hardware trigger that required a minimum total E_t summed over calorimeter towers in coincidence with at least one particle in each of the upstream and downstream scintillation counters. In the region $1.0 < |\eta| < 4.2$, only the electromagnetic calorimeters were included in the trigger. The E_t thresholds were set at 20, 30, 40, and 45 GeV depending on the luminosity. A total of 1.5×10^5 such triggers was recorded. Jets were identified according to a fixed-cone clustering algorithm¹⁰ with a cone size¹¹ of $\Delta R = 1.0$. The events were then required to have at least one jet with E_t greater than 20, 25, 40, or 40 GeV depending on the trigger threshold. In addition, the event vertex was required to be within 60 cm of the center of the detector along the beam axis. These criteria were satisfied by approximately 38 300 events.

Jets were required to have $0.1 < |\eta| < 0.8$, where η is the centroid in pseudorapidity as measured from the center of the detector. The energies of these jets were corrected¹⁰ for nonlinear calorimeter response, energy deposited in uninstrumented regions, energy lost outside the clustering cone, and the energy added from the "underlying event," i.e., that energy which is not associated with the hard parton scattering. The correction typically increased the jet E_t by 25%. The jets were then required to have corrected $E_t > 30$ GeV. Approximately 32 300 jets satisfied these criteria. The data sample is summarized in Table I.

The D^* search was performed using the standard scheme¹² where one looks for the decay sequence $D^{*+} \rightarrow D^0\pi^+$, $D^0 \rightarrow K^-\pi^+$ as well as the charge-conjugate modes. The small Q value in the D^* decay to $D^0\pi$ provides a powerful handle on background rejection. However, the combined branching ratio for the decay sequence is 2.4%¹³ so that, even with good reconstruction efficiency for D^* 's, one needs a large sample of jets to observe a D^* signal.

Charged-particle tracks in the CTC were reconstructed and constrained to the event vertex. The tracks were required to have $p_t > 0.3$ GeV/c and $|\eta| < 1.2$. Loose track-selection criteria based on the number of hits and the number of segments on the track were then applied. $K\pi$ and $K\pi\pi$ mass combinations were then formed where both kaon and pion assignments were tried for all tracks. To associate the $K\pi\pi$ system with a jet, the momentum of the system was required to be such that it was in the same hemisphere as a central jet. In cases of ambiguity, the closest jet in η - ϕ space was chosen.¹⁴ The following additional cuts were then applied (see Table II).

(1) For each $K\pi$ combination, we required $|M_{K\pi} - M_{D^0}| < 3\delta$, where δ is the uncertainty on $M_{K\pi}$ computed by propagating the track-parameter uncertainties (quoted earlier in this Letter) for the K and the π . δ differs slightly from 1 standard deviation in $M_{K\pi}$ because correlations between track parameters were ignored. For Monte Carlo D^* 's, δ ranges from 4 to 70 MeV/c² with a

TABLE I. The event sample used in this analysis, separated by triggers. The right-most column shows the average corrected E_t of the jets in each trigger sample.

Trigger threshold (GeV)	Number of events (10^3) after event selection	Number of jets (10^3) after jet selection	Average jet E_t (GeV)
20	1.6	0.7	39.0
30	28.4	23.8	42.7
40	4.0	3.7	58.8
45	4.3	4.1	59.7
Total	38.3	32.3	46.6

mean of $19 \text{ MeV}/c^2$.

(2) The polar angle of the kaon momentum vector in the D^0 rest frame was required to have $|\cos\theta^*| < 0.8$. This cut preferentially rejects background events since the typical opening angle between tracks in jets is small compared to the opening angle between the daughters of D^0 decays.

(3) The fractional momentum of the $K\pi\pi$ system, $z \equiv p_L(K\pi\pi)/E_{\text{jet}}$ (evaluated in the laboratory frame), was required to be greater than 0.1. The quantity $p_L(K\pi\pi)$ is the longitudinal component of the momentum of the $K\pi\pi$ system along the jet axis.

Figure 1(a) shows the mass difference $\Delta M = M_{K\pi\pi} - M_{K\pi}$ after all the cuts. A control sample, shown in the inset, is obtained from the "wrong-sign" mass combinations, i.e., $K^\pm \pi^\mp \pi^\pm$ with the same cuts. A clear excess is seen in the bin centered at $145.3 \text{ MeV}/c^2$, consistent with the world-average value for the $D^{*-}D^0$ mass difference of $145.45 \pm 0.07 \text{ MeV}/c^2$.¹⁵ As a further check of the background, the ΔM distribution for the "sidebands," where $3\delta < |M_{K\pi} - M_{D^0}| < 6\delta$, was examined. The distribution was found to be smooth and consistent with the wrong-sign distribution. To estimate the background under the peak, the ΔM distribution of Fig. 1(b) was fit to a Gaussian distribution in the peak region along with a background distribution parametrized as $a(\Delta M - m_\pi)^b$. Simultaneously, the fit was performed on

the wrong-sign distribution without the Gaussian term. Defining our D^* signal region by $144.5 < \Delta M < 146.5 \text{ MeV}/c^2$, we estimate that there are $25 D^{*\pm} \rightarrow K^\mp \pi^\pm \pi^\pm$ events on a background of 25 events, with a statistical uncertainty of ± 7.5 events. The systematic uncertainty on the background subtraction was estimated to be ± 2 events by fitting with and without the wrong-sign distribution and by varying the fitting function, the binning, and the region over which the fit was performed. For the distribution of Fig. 1(b) the parameters for the Gaussian are a mean of $145.2 \pm 0.2 \text{ MeV}/c^2$ and a σ of $0.56 \pm 0.18 \text{ MeV}/c^2$ where the uncertainties are statistical only. The width of the Gaussian is consistent with Monte Carlo expectations.

The efficiency was determined as a function of jet E_t , the fragmentation variable z , and the charged-particle multiplicity by reconstructing Monte Carlo D^* tracks which were injected into real jet data. Folding in the observed jet E_t spectrum, we obtained the efficiency as a function of z as shown in Fig. 2 for two values of the track multiplicity. The average efficiency for $z > 0.1$ was derived by folding in the observed z distribution for D^{*} 's, obtained by breaking up the ΔM distribution into (coarse) z bins and computing an excess of D^* events above background for each bin. For $z > 0.1$ an average efficiency of $(37 \pm 9)\%$ was obtained where the uncertainty is dominated by systematics. The major sources

TABLE II. The effect of the cuts applied to the tracks in this analysis. The efficiency of each of the cuts for D^{*} 's which were reconstructed with $z > 0.1$ is also listed.

	Number of track combinations	Efficiency for D^{*} 's ($z > 0.1$)
$p_t > 0.3 \text{ GeV}/c$, $ \eta < 1.2$...	0.85 ± 0.04
Track reconstruction	...	0.64 ± 0.10
$1500 < M_{K\pi} < 2400 \text{ MeV}/c^2$, $138 < \Delta M < 178 \text{ MeV}/c^2$	4.54×10^4	...
$ M_{K\pi} - M_{D^0} < 3\delta$, $144.5 < \Delta M < 146.5 \text{ MeV}/c^2$	90	0.78 ± 0.09
$ \cos\theta^* < 0.8$	61	0.84 ± 0.02
$z > 0.1$	50	...
After all cuts	50	0.37 ± 0.09

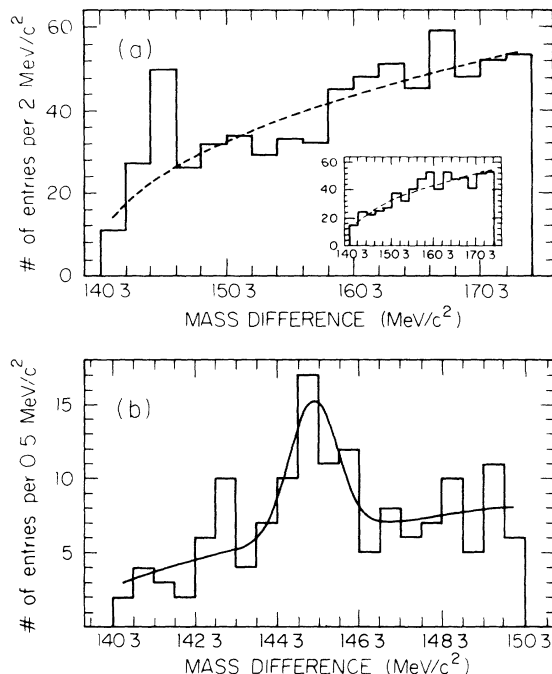


FIG. 1. (a) The mass difference $\Delta M \equiv M_{K\pi\pi} - M_{K\pi}$ after all the cuts. The dotted line is the same background function as shown in (b). Inset: The mass difference for the wrong-sign mass combinations, i.e., the combination $K^\pm \pi^\mp \pi^\pm$ instead of $K^\mp \pi^\pm \pi^\pm$. (b) The mass difference shown in finer detail in the region of the peak. The curve is a fit to a Gaussian distribution plus a background function parametrized as $a(\Delta M - m_\pi)^b$.

of uncertainty are our insufficient knowledge of the charged-particle multiplicity in events in which D^* 's are produced, and the uncertainty in the mass resolution for low-momentum D^* 's.

Using a Monte Carlo simulation, we estimate that the true number of events produced with $z > 0.1$ differs from the number observed by a multiplicative factor of 1.1 ± 0.2 due to the jet E_t resolution and the uncertainty in the jet energy scale. The uncertainty in the correction factor was estimated by varying the energy scale, the shape of the z distribution, and the magnitude of the jet E_t resolution.

To derive the number of $D^{*\pm}$ per jet, the number of $D^{*\pm} \rightarrow K^\mp \pi^\pm \pi^\pm$ decays observed was corrected for the efficiency (see Table II) and for the jet E_t resolution. Using the Mark III branching ratios,¹³ we obtain $N(D^{*\pm})/N(\text{jet}) = 0.10 \pm 0.03 \pm 0.03$ for D^* 's with $z > 0.1$ in jets with an average E_t of 47 GeV. This is consistent with previous measurements by the UA1 Collaboration^{3,4} at $\sqrt{s} = 546$ and 630 GeV for jets with an average E_t of 28 and 43 GeV, respectively. Estimates from QCD predict $N(D^{*\pm})/N(\text{jet})$ to be in the range 0.06–0.13 for 50-GeV gluon jets, where these predictions have been integrated over all values of z . To estimate the effect of our cut requiring $z > 0.1$ on this prediction we used the lowest-order formula for the z distribution of

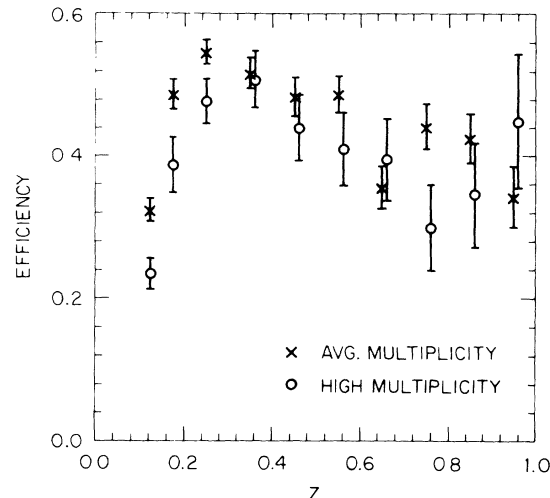


FIG. 2. The overall efficiency for D^* 's as a function of the fragmentation variable z for different track multiplicities in jets. The crosses show the efficiency for average jets and the open circles show the efficiency for jets with multiplicities typically 2 times higher.

charm quarks in gluon jets¹⁶ folded with parametrizations of charm fragmentation into D^* 's.¹⁷ We find that approximately 20% of the D^* 's are produced below our cut at $z = 0.1$. Although higher-order contributions are expected to increase this percentage, we conclude that QCD predictions are consistent with the measured results.

The observed D^* 's are concentrated at low values of z ; approximately 70% of the observed signal is between $z = 0.1$ and 0.2. Within the limited statistics, this is consistent with a previous UA1 measurement.³ As pointed out previously,³ the soft fragmentation function is different from that seen for D^* 's produced in e^+e^- collisions and can be interpreted as further evidence of the dominance of gluon splitting over gluon fusion for the production of charm in high- E_t jets.

We acknowledge the vital contribution of the members of the Fermilab accelerator division and the technical staffs of the participating institutions. We thank R. K. Ellis for useful discussions about the QCD calculations. This work was supported by the U.S. Department of Energy, the National Science Foundation, the Italian Istituto Nazionale di Fisica Nucleare, the Ministry of Science, Culture and Education of Japan, and the Alfred P. Sloan Foundation.

¹Z. Kunszt and E. Pietarinen, Nucl. Phys. **B164**, 45 (1980); V. Barger and R. J. N. Phillips, Phys. Rev. D **31**, 215 (1985); G. Köpp, J. H. Kühn, and P. M. Zerwas, Phys. Lett. **153B**, 315 (1985); F. Halzen and P. Hoyer, Phys. Lett. **154B**, 324 (1985); A. Ali and G. Ingelman, Phys. Lett. **156B**, 111 (1985).

²A. H. Mueller and P. Nason, Nucl. Phys. **B266**, 265 (1986).

³G. Arnison *et al.*, Phys. Lett. **147B**, 222 (1984).

⁴UA1 Collaboration, M. Ikeda *et al.*, in Proceedings of the Ninth Topical Workshop on Proton-Antiproton Physics, Castiglione, Italy, September 1989 (to be published).

⁵The parton-level cross sections can be found, for example, in J. F. Owens, E. Reya, and M. Glück, *Phys. Rev. D* **18**, 1501 (1978). The structure functions used were EHLQ set 1 from E. Eichten, I. Hinchliffe, K. Lane, and C. Quigg, *Rev. Mod. Phys.* **56**, 579 (1984). The momentum-transfer scale was taken to be $Q^2 = E_t^2$.

⁶The pseudorapidity is defined as $\eta = -\ln \tan(\theta/2)$, where θ is the polar angle.

⁷We have used the formulas of Ref. 2 for the number of charm quarks per gluon jet. The momentum-transfer scale was taken to be $Q^2 = E_t^2$. The charm-quark mass was varied from 1.2 to 1.8 GeV/c²; Λ_{QCD} was varied from 120 to 350 MeV. The probability that a charm quark materializes as a charged D^* was taken to be $\frac{3}{8}$ based on spin-counting the isospin invariance arguments. The value of $\frac{3}{8}$ is consistent with experimental measurements; see, for example, P. Avery *et al.*, *Phys. Rev. Lett.* **51**, 1139 (1983); M. Althoff *et al.*, *Phys. Lett.* **126B**, 493 (1983); W. Bartel *et al.*, *Phys. Lett.* **146B**, 121 (1984); H. Yamamoto *et al.*, *Phys. Rev. Lett.* **54**, 522 (1985); P. Baringer *et al.*, *Phys. Lett. B* **206**, 551 (1988).

⁸See F. Abe *et al.*, *Nucl. Instrum. Methods Phys. Res., Sect.*

A 271, 387 (1988), for a complete description and further references.

⁹R. D. St. Denis, Ph.D. thesis, Harvard University, 1988. The method used to determine the jet E_t resolution is outlined in P. Bagnaia *et al.*, *Phys. Lett.* **144B**, 283 (1984).

¹⁰F. Abe *et al.*, *Phys. Rev. Lett.* **62**, 613 (1989).

¹¹The cone size is the distance in η - ϕ space of a calorimeter tower from the jet axis, defined as $\Delta R \equiv [(\Delta\phi)^2 + (\Delta\eta)^2]^{1/2}$.

¹²S. Nussinov, *Phys. Rev. Lett.* **35**, 1672 (1975).

¹³We have used the latest branching ratios from Mark III: $B(D^{*+} \rightarrow D^0 \pi^+) = 0.57 \pm 0.04 \pm 0.04$ from J. Adler *et al.*, *Phys. Lett. B* **208**, 152 (1988), and $B(D^0 \rightarrow K^- \pi^+) = 0.042 \pm 0.004 \pm 0.004$ from J. Adler *et al.*, *Phys. Rev. Lett.* **60**, 89 (1988).

¹⁴At the end of the analysis, all the D^* candidates were found to be within $\Delta R = 1.0$ of the jet axis; 96% of the candidates were within $\Delta R = 0.7$.

¹⁵Particle Data Group, G. P. Yost *et al.*, *Phys. Lett. B* **204**, 1 (1988).

¹⁶R. K. Ellis, Fermilab Report No. Fermilab-Conf-89/168-T (to be published); in Proceedings of the Seventeenth SLAC Summer Institute, Stanford, California, July 1989 (to be published).

¹⁷See, for example, the references cited in Ref. 7.